IEEE Access
Multidisciplinary | Rapid Review | Open Access Journal

Received September 7, 2020, accepted September 22, 2020, date of publication September 25, 2020,
date of current version October 8, 2020.

Digital Object Identifier 10.1109/ACCESS.2020.3026786

A Three-Level Health Inspection Queue Based on Risk Screening Management Mechanism for Post-COVID Global Economic Recovery

CHIA-HUNG WANG, (Member, IEEE)
College of Information Science and Engineering, Fujian University of Technology, Fuzhou 350118, China
Fujian Provincial Key Laboratory of Big Data Mining and Applications, Fujian University of Technology, Fuzhou 350118, China

e-mail: jhwang728@hotmail.com

This work was supported in part by the Fujian Provincial Department of Science and Technology, China, under Grant 2016J01330, and in part by the Research Fund from the Fujian University of Technology under Grant GY-Z18148.

ABSTRACT Due to the serious impact of border control measures during the ongoing novel coronavirus (COVID-19) epidemic, new difficulties and challenges have been brought to the border lines of most countries and regions. Focusing on the post-COVID global economic recovery, we develop a computing method for studying the health inspection process based on a three-color risk screening management mechanism at border crossing checkpoints. In this article, to manage the cross-border risk efficiently during the epidemic prevention and control, we formulate a queueing model with hierarchical health inspection channels. The structural characteristics and properties of this three-level queueing model are also analyzed by studying the health inspection process with risk classification. Furthermore, we conduct a series of sensitivity analysis on several performance measures for the studied queueing system. In the numerical results, we figure out the monotonicity, convexity and complicated patterns of the derived formulas.

INDEX TERMS Queueing model, border control, operations management, system analysis and design, homeland security management, risk analysis, performance evaluation, epidemic prevention and control.

I. INTRODUCTION

The novel coronavirus disease, so-called COVID-19, has been declared a global pandemic by World Health Organization (WHO) since March 11, 2020. In order to prevent and control the severe situation of the ongoing COVID-19 epidemic, most countries and regions in the world have carried out strict border control measures [1]. For example, the inspectors and quarantine officers at airports, ports and land borders implement the health inspection and quarantine procedures, including entry quarantine, inspection and quantity control of carry-on items, screening and guiding isolation of abnormal travelers. For those abnormal travelers, the quarantine officers will evacuation them to designated isolation or medical places.

However, those epidemic prevention and control tasks related to border control have brought new difficulties and challenges to the global economic development [2]. The restrictive measures for cross-border flow of travelers have hindered the activities of international supply chain, and affected the industrial production of various regions. Therefore, it has become an important problem for optimizing the health inspection process at border crossing points.

In this article, we investigate a hierarchical inspection queueing process with three levels of inspection channels, which is of great significance to efficiently execute the border control management for releasing COVID-19 travelling restriction. Based on a three-color risk screening management mechanism, we are going to formulate a queueing model with hierarchical inspection channels. In addition, we will analyze the risk index and system performance of the studied three-level inspection queueing model. In the practical operation of border control and risk management, the efficiency of inspection services and the risk level are two dilemmatic goals to be achieved [3]–[5]. So, how to balance the risk and efficiency is a scientific problem worthy of study in the inspection process.

In general, there are two basic modes for inspection: uniform screening and selective screening. For uniform screening, we treat everyone with identical screening procedures;

The associate editor coordinating the review of this manuscript and approving it for publication was Qi Zhou.

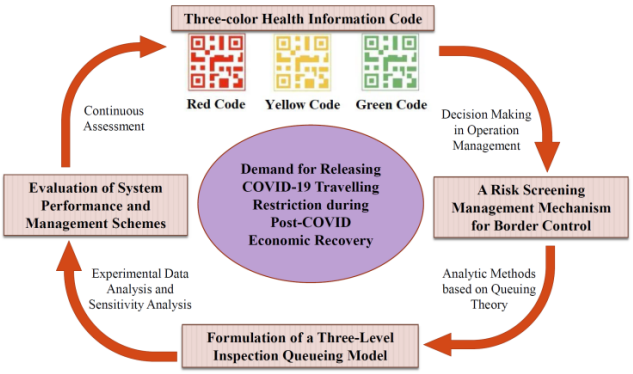

FIGURE 1. A flowchart for the present research.

however, for selective screening, we selectively apply inspection technologies and procedures on a targeted subgroup of people [6]–[9]. The uniform screening for COVID-19 virus has inevitably put hospitals and health systems in vulnerable positions, due to the shortages in medical capacity and resources to screen the whole people [10]. According to different system scenarios, many analytical tools were developed to study how to allocate security resources and identify where emphasis should be placed, e.g., [11]–[15]. According to the relevant information about persons to be screened, each of them can be assessed and given a corresponding risk value. Based on the assessed risk value of persons to be screened, the inspection system will assign him/her to the appropriate type of inspection channels.

However, when we are forced to expend resources to protect ourselves from COVID-19, we are reducing the resources available for investment, production and consumption of goods and services. In order to increase the likelihood of successfully managing emerging pandemics, it is important to consider valid population-based management approaches, decision-making, and continuous assessment [16]. It is also found that resources devoted to defense activities of any kind do not directly increase economic welfare [17], [18]. Besides, it is verified that long waiting time in the inspection queues has a negative impact on customer satisfaction [19]–[21]. Over the past decades, queueing theory has been applied extensively in the research works dedicated to the improvement in the security-check or inspection processes, such as [22]–[26]. Stochastic models can be used to estimate the performance of a queueing system in which the events are random [27], [28], and to identify the distribution of possible outcomes of a process (as in risk analysis) [29], [30].

The innovation of this article lies in the formulation of a three-level inspection queueing model based on the three-color risk screening management mechanism, which are a new phenomenon and an innovative method for border control under the current pandemic prevention and control. A flowchart for the present research is depicted in Fig. 1. In the present work, we aim to investigate the stochastic process of inspecting cross-border travelers by formulating a three-level inspection queueing model based on a health risk screening mechanism. The presented mathematical model and analysis provide a scientific tool which is necessary when exploring the border control policies for releasing cross-border travelling restriction and carrying out the management on the smooth flow of cross-border travelers. Taking into account both risk and inspection efficiency, we analyze the proposed queueing model and evaluate its system performance. The originality of this work is to provide an analytical method for the inspection management at border checkpoints, and the queueing analysis conducted in this article can be applied to meet the demand of border control on improving the efficiency of inspection service while ensuring the overall safety level.

The main contribution of this work is to present an executable queueing management scheme for health inspection process of cross-border travelers in order to achieve the goal of effectively optimizing the epidemic prevention and control at border checkpoints. The mathematical model presented in this article is useful as quantitative prescriptions of stochastic behaviors for making border control policies of government departments. It aims to provide information about the relationships among and relative importance of several factors influencing the studied queueing system. Besides, we reveal the stochastic behavior of the studied inspection queueing system through a series of computational experiments. For the post-COVID economic recovery, our research results would be useful in dredging the blocking points of inspection queues under the implementation of reopening the border lines.

The structure of this article is organized as follows. In Section II, we will introduce the health information code and a three-color risk screening management mechanism for reopening the border control under the current epidemic prevention control. The problem definitions and a three-level health inspection queueing system based on the three-color risk screening mechanism will be introduced in Section III. Next, in Section IV, we will give an illustrative example to demonstrate the proposed queueing analysis, and conduct a series of numerical experiments to reveal the performance evaluation of the studied queueing system. Finally, the concluding remarks are summarized in Section V.

II. A THREE-COLOR RISK SCREENING MANAGEMENT MECHANISM FOR RELEASING COVID-19 TRAVELLING RESTRICTION

The global economy is facing great challenges due to the serious impact of border control measures on the cross-border flow of international travelers. Strict health and quarantine measures have been enforced at points of entry and exit across the borders of most countries and regions to prevent inbound and outbound spread of the virus. The strictest-ever measures were applied at border control to suspend non-urgent and nonessential outbound travel by their citizens. Due to COVID-19 travelling restriction, it has impeded the cross-border flow of people, and delivered a blow to both the supply

chains and other economic activities, making a severe global economic recession unavoidable.

For the sake of our work and life gradually returning to normal, many countries/regions are looking for effective measures to lift inbound and outbound traffic restrictions during the battle against COVID-19. As of July 23, 2020, several countries have begun to gradually open the border for international travelers, such as the member states of European Union, United Kingdom, China, Thailand, Turkey, Ukraine, North Macedonia, Haiti, and so on.

Here, taking the measures implemented in China as an example, we introduce a three-color risk management mechanism to release the travelling restriction. In China, the government has launched "the epidemic prevention health information code" to implement the strategy of precise prevention and control at different risk levels [31]. As shown in Fig. 1, the health information code is divided into three color codes: Green code (low level of risk), Yellow code (medium level of risk), and Red code (high level of risk). A database for epidemic prevention health information code has been set up in accordance with the law to provide data services for COVID-19 risk control, and precisely identify different groups at risk.

In specific, the three-color risk management mechanism is based on the real health data and connects to relevant databases, such as the COVID-19 risk management system and control lists for travelling personnel. Through the online declaration and background review of an individual, it generates a color QR code belonging to him/her, which can be used as an electronic voucher for him/her to pass in and out. Thus, it can predict risk factors in different areas, and facilitate the orderly flow of people and the resumption of business operations.

With authorization from the public, the health information codes and digital travel records have been employed in China as permits for making trips. For example, when the travelers to be inspected enter the health inspection checkpoints, the three-color health information code belonging to an individual should be generated to mark his/her risk value by the risk pre-screening system. The health inspection personnel at the checkpoint will check the electronic voucher data of the travelers to be inspected, and then assign him/her to the appropriate inspection channel according to his/her risk level.

In summary, the three-color health information code can manage the flow of travelers efficiently for the economic recovery. The results shown on the health information code and historical records provide a base for the COVID-19 risk identification of cross-border travelers in different areas. In addition, the three-color health information code has made it possible to implement differentiated border control measures at different risk levels during the post-COVID global economic recovery. Therefore, it is essential to develop an analytical model that takes into account risk management and inspection efficiency under this three-color risk management mechanism.

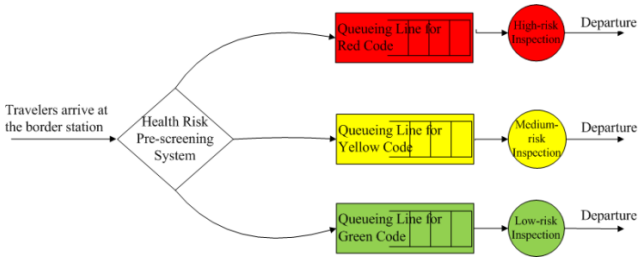

FIGURE 2. A three-level inspection queueing model for cross-border travelers under a three-color risk screening management mechanism.

III. A THREE-LEVEL HEALTH INSPECTION QUEUEING MODEL BASED ON RISK SCREENING MANAGEMENT

In this section, we present a three-level health inspection queueing model based on the three-color health information code, where the three-level inspection queues are studied based on a risk screening management mechanism. In the studied queueing system as shown in Fig. 2, two risk thresholds are to be used to distinguish those cross-border travelers for going through three different risk level inspection channels. We will formulate the queueing model and determine the performance measures of the entire queueing system with these two risk thresholds.

A. DEFINITIONS AND MODEL ASSUMPTIONS

As shown in Fig. 2, the health information provided by the database of a risk pre-screening system can be used to mark a risk value α for every cross-border traveler to be inspected at the border checkpoints, where the risk value α is a real number and lies between 0% and 100%. We assume that the risk value α of cross-border travelers to be inspected follows a probability density function $f(\alpha)$, and the risk value of each traveler is independent of each other.

Two risk thresholds τ_1 and τ_2 are used to distinguish the cross-border travelers between high-risk, medium-risk and low-risk classes. The values of risk thresholds τ_1 and τ_2 are real numbers between zero and one, and the value range is $0 \leq \tau_2 < \tau_1 \leq 1$. According to the assigned risk value α, the inspection officers will guide the travelers to be inspected to the corresponding queues of three level inspection channels.

It can be seen from Fig. 2 that the queueing process for inspecting cross-border travelers with three-level risk classification considered in this study is mainly divided into Red inspection channel (high level of risk), Yellow inspection channel (medium level of risk) and Green inspection channel (low level of risk). We represent s_1 as the number of inspectors (with equipment) set in Red inspection channel for high level of risk. In addition, the number of inspectors (with equipment) in the Yellow inspection channel for medium level of risk is expressed as s_2, and the number of inspectors (with equipment) in the Green inspection channel for low level of risk is denoted as s_3. Note that these three numbers s_1, s_2 and s_3 are positive integers.

Suppose that the inter-arrival time of cross-border travelers to be inspected follows the exponential distribution and is independent of each other, with the expected value of $1/\lambda$. The inspection time of three kinds of inspection channels follows an exponential distribution and is independent of each other. The expected inspection time of the Red inspection channel for high level of risk is $1/\mu_1$. The expected inspection time of the Yellow inspection channel for medium level of risk is $1/\mu_2$. The expected inspection time of the Green inspection channel for low level of risk is $1/\mu_3$. Compared with the other two inspection channels, the Red inspection channel has the longest inspection time and strictest quarantine, but the highest recognition rate for dangerous travelers. The Green inspection channel has the shortest inspection time and the highest service efficiency, but the lowest recognition rate for dangerous travelers.

If two risk thresholds τ_1 and τ_2 are given, the probability that the travelers to be inspected are assigned to the Red inspection channel can be expressed as $p_1(\tau_1, \tau_2)$. Meanwhile, the probability that the travelers to be inspected are assigned to the Yellow inspection channel can be expressed as $p_2(\tau_1, \tau_2)$, and the probability that the travelers to be inspected are assigned to the Green inspection channel can be expressed as $p_1(\tau_1, \tau_2)$. Note that it is obvious that the following condition holds:

$$p_1(\tau_1, \tau_2) + p_2(\tau_1, \tau_2) + p_3(\tau_1, \tau_2) = 1. \tag{1}$$

In the next subsection, we are going to formulate a queueing model based on a three-color risk management mechanism, which can be used to evaluate the system performance in the cross-border inspection process. The queue discipline is first come, first served, where travelers are inspected in the same order in which they arrive at the checkpoint. The mathematical notations and definitions of the queueing model studied in this article are summarized in Table 1.

B. A QUEUEING ANALYSIS

The independence of arrivals in disjoint time intervals together with the memoryless property of the exponential service time distribution implies that the counting number of cross-border travelers to be inspected at the three-level health inspection queueing system forms a time homogeneous Markov chain, in particular, a birth and death process.

Under the condition of risk thresholds $0 \le \tau_2 < \tau_1 \le 1$, the probability that the travelers to be inspected are assigned to the Green inspection channel for low level of risk can be derived as:

$$p_3(\tau_1, \tau_2) = \int_0^{\tau_2} f(\alpha) d\alpha, \tag{2}$$

and the probability that the travelers to be inspected are assigned to the Red inspection channel for medium level of risk can be derived as:

$$p_1(\tau_1, \tau_2) = \int_{\tau_1}^{1} f(\alpha) d\alpha. \tag{3}$$

TABLE 1. Definitions of mathematical notations for the health inspection queueing model.

Notation	Definition
λ	The average arrival rate of cross-border travelers to be inspected.
α	The risk value of travelers to be inspected, which is a random variable between 0% and 100%.
τ_1	The risk threshold for distinguishing high-risk travelers and medium-risk travelers.
τ_2	The risk threshold for distinguishing medium-risk travelers and low-risk travelers.
μ_1	The average service rate at the Red inspection channel for high level of risk.
μ_2	The average service rate at the Yellow inspection channel for medium level of risk.
μ_3	The average service rate at the Green inspection channel for low level of risk.
s_1	The number of inspectors (with equipment) at the Red inspection channel.
s_2	The number of inspectors (with equipment) at the Yellow inspection channel.
s_3	The number of inspectors (with equipment) at the Green inspection channel.
d_1	The recognition rate for inspection and quarantine at the Red inspection channel, which is a constant number between 0% and 100%.
d_2	The recognition rate for inspection and quarantine at the Yellow inspection channel, which is a constant number between 0% and 100%.
d_3	The recognition rate for inspection and quarantine at the Green inspection channel, which is a constant number between 0% and 100%.
$p_1(\tau_1, \tau_2)$	The probability of cross-border travelers assigned to the Red inspection channel.
$p_2(\tau_1, \tau_2)$	The probability of cross-border travelers assigned to the Yellow inspection channel.
$p_3(\tau_1, \tau_2)$	The probability of cross-border travelers assigned to the Green inspection channel.
$R_1(\tau_1, \tau_2)$	The risk ratio of cross-border travelers assigned to the Red inspection channel.
$R_2(\tau_1, \tau_2)$	The risk ratio of cross-border travelers assigned to the Yellow inspection channel.
$R_3(\tau_1, \tau_2)$	The risk ratio of cross-border travelers assigned to the Green inspection channel.
Performance Measure of the Queueing System	
$W(\tau_1, \tau_2, s_1, s_2, s_3)$	The average time spent by a cross-border traveler at the health inspection queueing system given the risk thresholds τ_1, τ_2 and the numbers of inspectors s_1, s_2, s_3.
$L(\tau_1, \tau_2, s_1, s_2, s_3)$	The average number of cross-border travelers at the health inspection queueing system given the risk thresholds τ_1, τ_2 and the numbers of inspectors s_1, s_2, s_3.
$SL(\tau_1, \tau_2)$	The safety level of the overall health inspection queueing system given the risk thresholds τ_1 and τ_2.

Thus, we can determine the probability that the travelers to be inspected are assigned to the Yellow inspection channel

for high level of risk:

$$p_2(\tau_1,\tau_2) = 1 - p_3(\tau_1,\tau_2) - p_1(\tau_1,\tau_2) = \int_{\tau_2}^{\tau_1} f(\alpha)d\alpha. \quad (4)$$

For the Red inspection channel, we denote $X^{(R)}(t)$ as the number of cross-border travelers waiting in the Red inspection channel at time t. When a fixed number s_1 of inspectors (with equipment) are available in the Red inspection channel, then $X^{(R)}(t)$ forms a birth and death process with birth parameters

$$\lambda_n^{(R)} = p_1(\tau_1,\tau_2)\cdot\lambda, \quad \text{for } n = 0, 1, \ldots, \quad (5)$$

and death parameters

$$\mu_n^{(R)} = \begin{cases} n\cdot\mu_1, & \text{for } n = 0, 1, \ldots, s_1, \\ s_1\cdot\mu_1, & \text{for } n > s_1. \end{cases} \quad (6)$$

Then the number undergoing the inspection service is $\min\left\{X^{(R)}(t), s_1\right\}$, and the number waiting for service is $\max\left\{X^{(R)}(t) - s_1, 0\right\}$. Besides, we can denote the traffic intensity of the Red inspection channel as

$$\rho_1 = \frac{p_1(\tau_1,\tau_2)\cdot\lambda}{s_1\cdot\mu_1}. \quad (7)$$

Note that, as the traffic intensity ρ_1 approaches one, the mean queue length in the Red inspection channel becomes unbounded. Let

$$\pi_n^{(R)} = \lim_{t\to\infty}\Pr\{X^{(R)}(t) = n\}, \quad \text{for } n = 0, 1, \ldots, \quad (8)$$

be the equilibrium distribution of queue length in the Red inspection channel. When it holds the stability condition that $\rho_1 < 1$, we can determine

$$\pi_0^{(R)} = \left\{\sum_{j=0}^{s_1-1}\frac{(s_1\cdot\rho_1)^j}{j!} + \frac{(s_1\cdot\rho_1)^{s_1}}{s_1!\cdot(1-\rho_1)}\right\}^{-1}, \quad (9)$$

and

$$\pi_n^{(R)} = \begin{cases} \dfrac{(s_1\cdot\rho_1)^n}{n!}\cdot\pi_0^{(R)}, & \text{for } n = 0, 1, \ldots, s_1 \\ \dfrac{(s_1\cdot\rho_1)^{s_1}}{s_1!}\cdot\rho_1^{n-s_1}\cdot\pi_0^{(R)}, & \text{for } n \geq s_1 \end{cases} \quad (10)$$

For the Yellow inspection channel, we denote $X^{(Y)}(t)$ as the number of cross-border travelers waiting in the Yellow inspection channel at time t. When a fixed number s_2 of inspectors (with equipment) are available in the Yellow inspection channel, then the appropriate birth and death parameters are

$$\lambda_n^{(Y)} = p_2(\tau_1,\tau_2)\cdot\lambda, \quad \text{for } n = 0, 1, \ldots, \quad (11)$$

and

$$\mu_n^{(Y)} = \begin{cases} n\cdot\mu_2, & \text{for } n = 0, 1, \ldots, s_2, \\ s_2\cdot\mu_2, & \text{for } n > s_2. \end{cases} \quad (12)$$

In addition, the number undergoing the inspection service of the Yellow inspection channel is $\min\left\{X^{(Y)}(t), s_2\right\}$, and the number waiting for service is $\max\left\{X^{(Y)}(t) - s_2, 0\right\}$. Next, we denote the traffic intensity of the Yellow inspection channel as

$$\rho_2 = \frac{p_2(\tau_1,\tau_2)\cdot\lambda}{s_2\cdot\mu_2}. \quad (13)$$

Under the stability condition that $\rho_2 < 1$, we can derive the equilibrium distribution

$$\pi_0^{(Y)} = \left\{\sum_{j=0}^{s_2-1}\frac{(s_2\cdot\rho_2)^j}{j!} + \frac{(s_2\cdot\rho_2)^{s_2}}{s_2!\cdot(1-\rho_2)}\right\}^{-1}, \quad (14)$$

and

$$\pi_n^{(Y)} = \begin{cases} \dfrac{(s_2\cdot\rho_2)^n}{n!}\cdot\pi_0^{(Y)}, & \text{for } n = 0, 1, \ldots, s_2 \\ \dfrac{(s_2\cdot\rho_2)^{s_2}}{s_2!}\cdot\rho_2^{n-s_2}\cdot\pi_0^{(Y)}, & \text{for } n \geq s_2 \end{cases} \quad (15)$$

Similarly, for the Green inspection channel, we denote $X^{(G)}(t)$ as the number of cross-border travelers waiting in the Green inspection channel at time t. When a fixed number s_3 of inspectors (with equipment) are available in the Green inspection channel, then the appropriate birth and death parameters are

$$\lambda_n^{(G)} = p_3(\tau_1,\tau_2)\cdot\lambda, \quad \text{for } n = 0, 1, \ldots, \quad (16)$$

and

$$\mu_n^{(G)} = \begin{cases} n\cdot\mu_3, & \text{for } n = 0, 1, \ldots, s_3, \\ s_3\cdot\mu_3, & \text{for } n > s_3. \end{cases} \quad (17)$$

Furthermore, the number undergoing the inspection service of the Green inspection channel is $\min\left\{X^{(G)}(t), s_3\right\}$, and the number waiting for service is $\max\left\{X^{(G)}(t) - s_3, 0\right\}$. Next, we denote the traffic intensity of the Green inspection channel as

$$\rho_3 = \frac{p_3(\tau_1,\tau_2)\cdot\lambda}{s_3\cdot\mu_3}. \quad (18)$$

If it holds the stability condition that $\rho_3 < 1$, we can derive the equilibrium distribution

$$\pi_0^{(G)} = \left\{\sum_{j=0}^{s_3-1}\frac{(s_3\cdot\rho_3)^j}{j!} + \frac{(s_3\cdot\rho_3)^{s_3}}{s_3!\cdot(1-\rho_3)}\right\}^{-1}, \quad (19)$$

and

$$\pi_n^{(G)} = \begin{cases} \dfrac{(s_3\cdot\rho_3)^n}{n!}\cdot\pi_0^{(G)}, & \text{for } n = 0, 1, \ldots, s_3 \\ \dfrac{(s_3\cdot\rho_3)^{s_3}}{s_3!}\cdot\rho_3^{n-s_3}\cdot\pi_0^{(G)}, & \text{for } n \geq s_3 \end{cases} \quad (20)$$

The equilibrium distributions (9), (10), (14), (15), (19) and (20) can demonstrate the limiting behavior of the studied queueing system. Besides, these equilibrium distributions

enable us to calculate the major system performance measures, such as the expected number of travelers in the studied queueing system and the average time spent by each cross-border traveler.

C. PERFORMANCE MEASURE OF THE QUEUEING SYSTEM

Here, we are going to derive three major performance measures for the proposed three-level inspection queueing model, including the average system size, the average time spent in the system, and the safety level of the overall system.

When the studied queueing system operates sufficiently long to have reached an appropriate steady state, we can evaluate the average queue size and average waiting time with the equilibrium distributions. With the equilibrium distributions (9) and (10), we can calculate $L_q^{(R)}$, the average number of travelers in the system waiting for (and not undergoing) the inspection service at the Red inspection channel as follows:

$$L_q^{(R)} = \sum_{n=s_1}^{\infty} (n - s_1) \cdot \pi_n^{(R)} = \frac{s_1^{s_1} \cdot \rho_1^{s_1+1}}{s_1! \cdot (1-\rho_1)^2} \cdot \pi_0^{(R)}. \quad (21)$$

Then, with the help of Little's formula, we can determine the average time spent by a traveler with high level of risk in the queue line

$$W_q^{(R)} = \frac{L_q^{(R)}}{p_1(\tau_1, \tau_2) \cdot \lambda}, \quad (22)$$

and the average time spent for passing through the Red inspection channel

$$W^{(R)} = W_q^{(R)} + \frac{1}{\mu_1}. \quad (23)$$

Thus, we determine the average number of travelers with high level of risk in the whole queueing system

$$L^{(R)} = p_1(\tau_1, \tau_2) \cdot \lambda \cdot W^{(R)} = L_q^{(R)} + s_1 \cdot \rho_1. \quad (24)$$

With the equilibrium distributions (14) and (15), we determine $L_q^{(Y)}$, the average number of travelers in the system waiting for (and not undergoing) the inspection service at the Yellow inspection channel as follows:

$$L_q^{(Y)} = \sum_{n=s_2}^{\infty} (n - s_2) \cdot \pi_n^{(Y)} = \frac{s_2^{s_2} \cdot \rho_2^{s_2+1}}{s_2! \cdot (1-\rho_2)^2} \cdot \pi_0^{(Y)}. \quad (25)$$

Then, with the help of Little's formula, we can determine the average time spent by a traveler with medium level of risk in the queue line

$$W_q^{(Y)} = \frac{L_q^{(Y)}}{p_2(\tau_1, \tau_2) \cdot \lambda}, \quad (26)$$

and the average time spent for passing through the Yellow inspection channel

$$W^{(Y)} = W_q^{(Y)} + \frac{1}{\mu_2}. \quad (27)$$

Thus, we obtain the average number of travelers with medium level of risk in the whole queueing system

$$L^{(Y)} = p_2(\tau_1, \tau_2) \cdot \lambda \cdot W^{(Y)} = L_q^{(Y)} + s_2 \cdot \rho_2. \quad (28)$$

With the equilibrium distributions (19) and (20), we can evaluate $L_q^{(G)}$, the average number of travelers in the system waiting for (and not undergoing) the inspection service at the Green inspection channel as follows:

$$L_q^{(G)} = \sum_{n=s_3}^{\infty} (n - s_3) \cdot \pi_n^{(G)} = \frac{s_3^{s_3} \cdot \rho_3^{s_3+1}}{s_3! \cdot (1-\rho_3)^2} \cdot \pi_0^{(G)}. \quad (29)$$

Then, with the help of Little's formula, we can determine the average time spent by a traveler with low level of risk in the queue line

$$W_q^{(G)} = \frac{L_q^{(G)}}{p_3(\tau_1, \tau_2) \cdot \lambda}, \quad (30)$$

and the average time spent for passing through the Green inspection channel

$$W^{(G)} = W_q^{(G)} + \frac{1}{\mu_3}. \quad (31)$$

Thus, we obtain the average number of travelers with low level of risk in the whole queueing system

$$L^{(G)} = p_3(\tau_1, \tau_2) \cdot \lambda \cdot W^{(G)} = L_q^{(G)} + s_3 \cdot \rho_3. \quad (32)$$

After determining the values of $W^{(R)}$, $W^{(Y)}$ and $W^{(G)}$, we can obtain an important performance measure for the health inspection queueing system, that is, the average time spent by a cross-border traveler at the health inspection queueing system, $W(\tau_1, \tau_2, s_1, s_2, s_3)$. Given the risk thresholds τ_1, τ_2 and the numbers of inspectors s_1, s_2, s_3, we have the following equation:

$$\begin{aligned} &W(\tau_1, \tau_2, s_1, s_2, s_3) \\ &\quad = p_1(\tau_1, \tau_2) \cdot W^{(R)} + p_2(\tau_1, \tau_2) \cdot W^{(Y)} \\ &\qquad + p_3(\tau_1, \tau_2) \cdot W^{(G)}. \end{aligned} \quad (33)$$

In addition, with the values of $L^{(R)}$, $L^{(Y)}$ and $L^{(G)}$, we can also obtain the average number of cross-border travelers at the health inspection queueing system, $L(\tau_1, \tau_2, s_1, s_2, s_3)$. Given the risk thresholds τ_1, τ_2 and the numbers of inspectors s_1, s_2, s_3, we have the second performance measure for the health inspection queueing system, $L(\tau_1, \tau_2, s_1, s_2, s_3)$, which is derived in the following equation:

$$\begin{aligned} &L(\tau_1, \tau_2, s_1, s_2, s_3) \\ &\quad = p_1(\tau_1, \tau_2) \cdot L^{(R)} + p_2(\tau_1, \tau_2) \cdot L^{(Y)} \\ &\qquad + p_3(\tau_1, \tau_2) \cdot L^{(G)}. \end{aligned} \quad (34)$$

Furthermore, if it is given that $0 \le \tau_2 < \tau_1 \le 1$, we can derive the risk ratio of travelers assigned to the Green inspection channel is:

$$R_3(\tau_1, \tau_2) = \frac{\int_0^{\tau_2} \alpha \cdot f(\alpha) d\alpha}{\int_0^1 \alpha \cdot f(\alpha) d\alpha}, \quad (35)$$

where $f(\alpha)$ is a probability density function of the risk value α for those cross-border travelers to be inspected. In addition,

the risk ratio of travelers assigned to the Red inspection channel is:

$$R_1(\tau_1, \tau_2) = \frac{\int_{\tau_1}^{1} \alpha \cdot f(\alpha) d\alpha}{\int_{0}^{1} \alpha \cdot f(\alpha) d\alpha}. \quad (36)$$

Therefore, from the condition (1), we can determine the risk ratio of travelers assigned to the Yellow inspection channel as follows:

$$\begin{aligned} R_2(\tau_1, \tau_2) &= 1 - R_3(\tau_1, \tau_2) - R_1(\tau_1, \tau_2) \\ &= \frac{\int_{\tau_2}^{\tau_1} \alpha \cdot f(\alpha) d\alpha}{\int_{0}^{1} \alpha \cdot f(\alpha) d\alpha}. \end{aligned} \quad (37)$$

Finally, we denote $SL(\tau_1, \tau_2)$ as the safety level of the overall health inspection queueing system given the risk thresholds τ_1 and τ_2. With the values of three risk ratios $R_1(\tau_1, \tau_2)$, $R_2(\tau_1, \tau_2)$ and $R_3(\tau_1, \tau_2)$, we can determine the safety level of the overall health inspection queueing system as follows:

$$SL(\tau_1, \tau_2) = \sum_{i=1}^{3} d_i \cdot R_i(\tau_1, \tau_2), \quad (38)$$

where d_i is the recognition rate for inspection and quarantine at the corresponding inspection channel, which is a constant number between 0% and 100%. The safety level, $SL(\tau_1, \tau_2)$, is the third performance measure for the overall health inspection queueing system.

IV. NUMERICAL RESULTS

In this section, we demonstrate the proposed approach through solving an illustrative example, and conduct a sensitivity analysis on the studied queueing system through a series of numerical experiments to figure out the effects of varying two risk thresholds on the presented three performance measures. Besides, a special case when two risk thresholds are identical is also presented as an application of our model.

A. PARAMETER SETTINGS

The parameter settings given here are used to provide a numerical example of our calculation process in Section III, and the different setting of model parameters will not change the correctness of those derived formulas in the present paper. The parameter settings of the illustrative example are given as follows. The average arrival rate is $\lambda = 5$ travelers per minute. The numbers of inspectors (with equipment) set in three levels of inspection channels are given as $s_1 = 5$, $s_2 = 3$, and $s_3 = 2$. Meanwhile, the recognition rates at those three levels of inspection channels are given as $d_1 = 99\%$, $d_2 = 80\%$, and $d_3 = 75\%$, and the average service rate for each level of inspection channel is set as $\mu_1 = 1.0$ (traveler/minute), $\mu_2 = 1.5$ (traveler/minute), and $\mu_3 = 2.6$ (traveler/minute), individually. Besides, two risk thresholds τ_1 and τ_2 are varied within the interval [0%, 100%], i.e., $0 \le \tau_2 < \tau_1 \le 1$.

Moreover, as an illustrative example taken from [20], it is given that the risk value α of the travelers to be inspected follows a truncated exponential distribution, and each risk value is independent of each other. The probability density function of a truncated exponential distribution is given as follows:

$$f(\alpha \mid \theta) = \frac{e^{-\alpha/\theta}}{\theta(1 - e^{-1/\theta})}, \quad 0 < \alpha \le 1, \quad (39)$$

where θ is the parameter of the truncated exponential distribution. Therefore, the average risk value $E[\alpha]$ of travelers to be inspected can be expressed as follows:

$$E[\alpha] = \int_0^1 \alpha \cdot f(\alpha \mid \theta) d\alpha = \theta - \frac{e^{-1/\theta}}{1 - e^{-1/\theta}} \approx \theta. \quad (40)$$

That is, the average risk value $E[\alpha]$ is approximately the parameter θ of the truncated exponential distribution. According to the statistics of McLay *et al.* [32], we take $\theta = 0.0625$ as the parameter of truncated exponential distribution in the numerical experiments.

Our computational environment is run by means of MATLAB 2017a on Windows 10 Professional 64-bit with the processor Intel (R) Core (TM) i7-6500U CPU@2.50GHz dual-core and 8 GB memory.

B. AN ILLUSTRATIVE EXAMPLE

Given $0 \le \tau_2 < \tau_1 \le 1$, we can derive the probability that those cross-border travelers are to be assigned to the Green inspection channel

$$p_3(\tau_1, \tau_2) = \int_0^{\tau_2} f(\alpha \mid \theta) d\alpha = \frac{1 - e^{-\tau_2/\theta}}{1 - e^{-1/\theta}},$$

and the probability that those cross-border travelers are to be assigned to the Red inspection channel

$$p_1(\tau_1, \tau_2) = \int_{\tau_1}^{1} f(\alpha \mid \theta) d\alpha = \frac{e^{-\tau_1/\theta} - e^{-1/\theta}}{1 - e^{-1/\theta}}.$$

With the help of condition (1), we can easily determine the probability that those cross-border travelers are to be assigned to the Yellow inspection channel as follows:

$$p_2(\tau_1, \tau_2) = 1 - p_3(\tau_1, \tau_2) - p_1(\tau_1, \tau_2) = \frac{e^{-\tau_2/\theta} - e^{-\tau_1/\theta}}{1 - e^{-1/\theta}}.$$

After obtaining the above three probabilities, we can evaluate the traffic intensities $\rho_1 = p_1(\tau_1, \tau_2)$, $\rho_2 = {}^{10}/_{9} \cdot p_2(\tau_1, \tau_2)$ and $\rho_3 = {}^{25}/_{26} \cdot p_3(\tau_1, \tau_2)$ via the equations (7), (13) and (18). Moreover, when it holds the stability conditions, the equilibrium distributions $\pi_n^{(G)}$, $\pi_n^{(Y)}$, and $\pi_n^{(R)}$ can be determined by using equations (9), (10), (14), (15), (19) and (20). Therefore, two important performance measures can be easily obtained via the equations (33) and (34), that is, the average time $W(\tau_1, \tau_2, s_1, s_2, s_3)$ spent by a cross-border traveler and the average number $L(\tau_1, \tau_2, s_1, s_2, s_3)$ at the health inspection queueing system.

Furthermore, from the equations (35) and (36), we can derive the risk ratio of travelers assigned to the Green inspection channel

$$\begin{aligned} R_3(\tau_1, \tau_2) &= \frac{\int_0^{\tau_2} \alpha \cdot f(\alpha \mid \theta) d\alpha}{\int_0^1 \alpha \cdot f(\alpha \mid \theta) d\alpha} \\ &= \frac{\tau_2 \cdot e^{-\tau_2/\theta} + \theta \cdot e^{-\tau_2/\theta} - \theta}{e^{-1/\theta} + \theta \cdot e^{-1/\theta} - \theta}, \end{aligned}$$

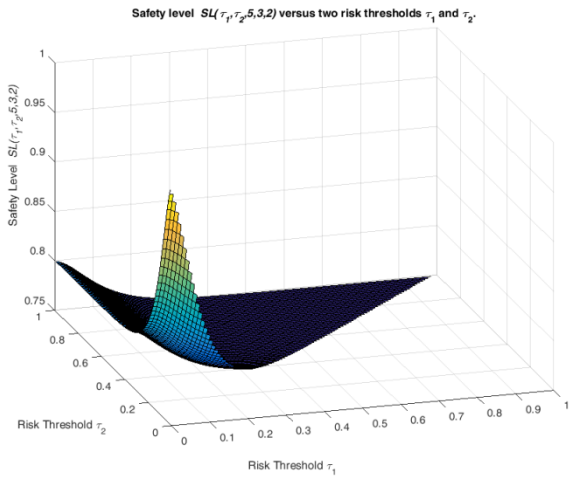

FIGURE 3. A 3D diagram for the safety level $\mathbf{SL}(\tau_1, \tau_2)$ of two risk thresholds τ_1 and τ_2 given the parameter settings $s_1 = 5$, $s_2 = 3$ and $s_3 = 2$.

and the risk ratio of travelers assigned to the Red inspection channel

$$R_1(\tau_1, \tau_2) = \frac{\int_{\tau_1}^{1} \alpha \cdot f(\alpha \mid \theta)\, d\alpha}{\int_{0}^{1} \alpha \cdot f(\alpha \mid \theta)\, d\alpha} = \frac{e^{-1/\theta} - \tau_1 \cdot e^{-\tau_1/\theta} + \theta \cdot e^{-1/\theta} - \theta \cdot e^{-\tau_1/\theta}}{e^{-1/\theta} + \theta \cdot e^{-1/\theta} - \theta},$$

where it is given that $0 \leq \tau_2 < \tau_1 \leq 1$. So, with the help of condition (1), we can easily determine the risk ratio of travelers assigned to the Yellow inspection channel as follows:

$$R_2(\tau_1, \tau_2) = 1 - R_3(\tau_1, \tau_2) - R_1(\tau_1, \tau_2) = \frac{\tau_1 \cdot e^{-\tau_1/\theta} + \theta \cdot e^{-\tau_1/\theta} - \tau_2 \cdot e^{-\tau_2/\theta} - \theta \cdot e^{-\tau_2/\theta}}{e^{-1/\theta} + \theta \cdot e^{-1/\theta} - \theta}.$$

After obtaining the above three risk ratios, we can determine the last performance measure via the equation (38), i.e., the safety level $SL(\tau_1, \tau_2)$ for the overall health inspection queueing system.

Next, we observe the effects of varying two risk thresholds τ_1 and τ_2 on the studied three performance measures under the parameter settings $s_1 = 5$, $s_2 = 3$ and $s_3 = 2$. From Fig. 3 to Fig. 5, it illustrates the numerical results of the average waiting time $\mathrm{W}(\tau_1, \tau_2, 5, 3, 2)$, the average number $\mathrm{L}(\tau_1, \tau_2, 5, 3, 2)$, and the safety level $\mathrm{SL}(\tau_1, \tau_2)$ when varying two risk thresholds τ_1 and τ_2 in the domain range $0 \leq \tau_2 < \tau_1 \leq 1$.

In Fig. 3, it shows that the safety level $SL(\tau_1, \tau_2)$ is decreasing when we enlarge two risk thresholds. In Fig. 4 and Fig. 5, we find that the surface of average number $L(\tau_1, \tau_2, 5, 3, 2)$ and average time $W(\tau_1, \tau_2, 5, 3, 2)$ are decreasing when two risk thresholds lies in a small region near the origin point (0,0), while the function values will become increasing as enlarging two risk thresholds outside this small region.

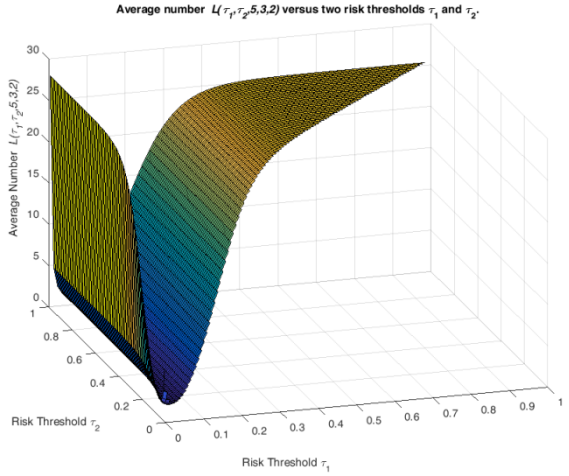

FIGURE 4. A 3D diagram for the average number $\boldsymbol{L}(\tau_1, \tau_2, s_1, s_2, s_3)$ of two risk thresholds τ_1 and τ_2 given the parameter settings $s_1 = 5$, $s_2 = 3$ and $s_3 = 2$.

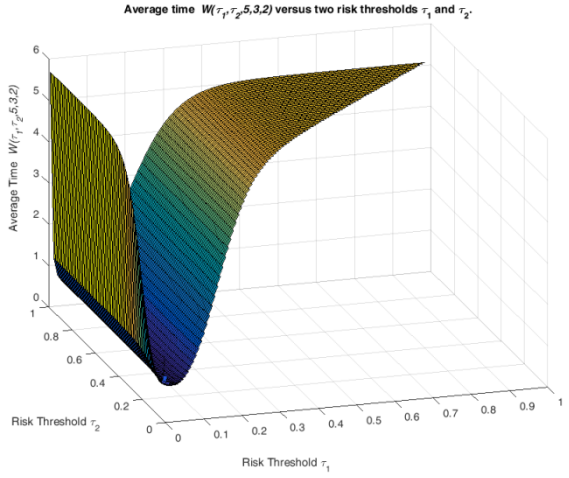

FIGURE 5. A 3D diagram for the average time $\boldsymbol{W}(\tau_1, \tau_2, s_1, s_2, s_3)$ of two risk thresholds τ_1 and τ_2 given the parameter settings $s_1 = 5$, $s_2 = 3$ and $s_3 = 2$.

C. A SPECIAL CASE WHEN TWO RISK THRESHOLDS ARE IDENTICAL

In this subsection, we demonstrate that our three-level health inspection queueing model can be simplified to an inspection queueing model with two types of inspection channels and only one risk threshold. When two risk thresholds τ_1 and τ_2 are identical, it is obvious that the probability that those cross-border travelers are to be assigned to the Yellow inspection channel will become zero, i.e., $p_2(\tau_1, \tau_2) = 0$. In such a special case, the proposed three-level inspection queueing model can be reduced to a two-level inspection queueing model consists of Red inspection channel (for higher level of risk) and Green inspection channel (for lower level of risk). That is, in the case when $\tau_1 = \tau_2$, there is only two-level risk classification for cross-border travelers, and there is only one risk threshold used in this simpler inspection queueing system.

Next, we investigate the effects of changing a risk threshold on such a simplified inspection queueing system with only

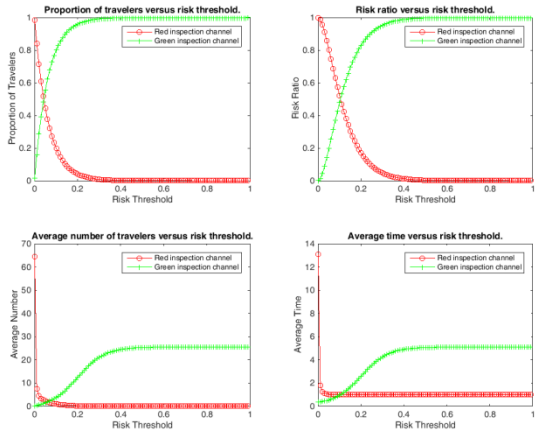

FIGURE 6. Four performance indices for two types of inspection channels when varying the risk threshold between 0% and 100%.

two types of inspection channels. For the simplification of notation, we take $\tau = \tau_1 = \tau_2$ in the following derivation. Given $0 \leq \tau \leq 1$, we can derive the probability that the cross-border travelers are to be assigned to the Green inspection channel

$$p_3(\tau) = \int_0^{\tau} f(\alpha \mid \theta)\, d\alpha = \frac{1 - e^{-\tau/\theta}}{1 - e^{-1/\theta}},$$

and the probability that those cross-border travelers are to be assigned to the Red inspection channel

$$p_1(\tau) = 1 - p_G(\tau) = \frac{e^{-\tau/\theta} - e^{-1/\theta}}{1 - e^{-1/\theta}}.$$

Therefore, under the stability conditions $\rho_1 = p_1(\tau) < 1$ and $\rho_3 = {}^{25}/_{26} \cdot p_3(\tau) < 1$, we can determine the average time spent for passing through the Red inspection channel, $W^{(R)}$, and the average time spent for passing through the Green inspection channel, $W^{(G)}$, via equations (23) and (31). In addition, we can also calculate the average number of travelers with lower level of risk in the two-level inspection queueing system, $L^{(G)}$, and the average number of travelers with higher level of risk in the system, $L^{(R)}$, via equations (24) and (32). Furthermore, from the equations (35) and (36), we can derive the risk ratio of travelers assigned to the Green inspection channel, $R_3(\tau)$, and the risk ratio of travelers assigned to the Red inspection channel, $R_1(\tau)$. Finally, we obtain three major performance measures for the two-level inspection queueing, such as the average time $W(\tau, s_1, s_3)$, the average number $L(\tau, s_1, s_3)$, and the safety level $SL(\tau)$. The numerical results of the derived performance measures are illustrated in Figs. 6-9 under the parameter settings $\lambda = 5$, $s_1 = 5$, and $s_3 = 2$.

When varying the risk threshold τ between 0% and 100%, Fig. 6 illustrates four performance indices for two types of inspection channels, including the probability of travelers assigned to each type of inspection channel, the risk ratio, the average time, and the average number of travelers. For a closer insight into the curves of changes, Fig. 7 shows those numerical results especially when the risk threshold lies in

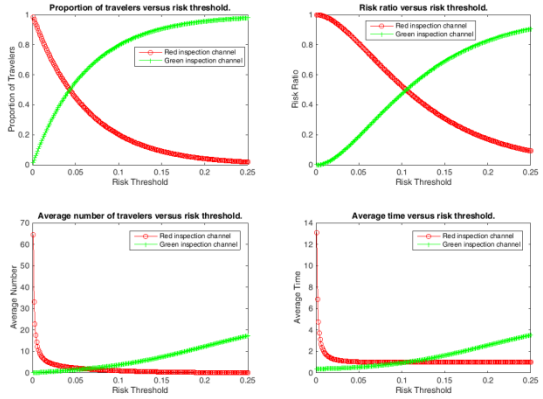

FIGURE 7. Four performance indices for two types of inspection channels when varying the risk threshold between 0% and 25%.

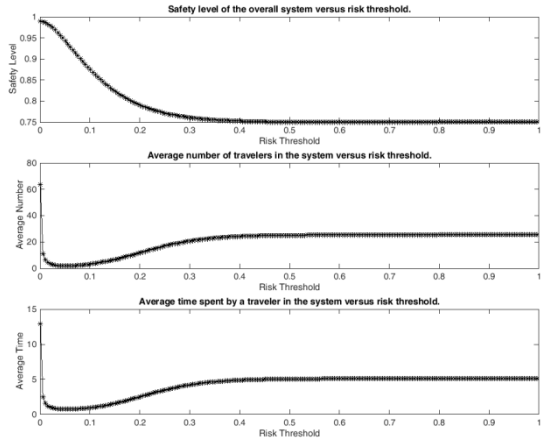

FIGURE 8. Three performance indices for a two-level inspection queueing system when varying the risk threshold between 0% and 100%.

the interval $[0\%, 25\%]$. It can be found that the probability $p_3(\tau)$ increases and the probability $p_1(\tau)$ decreases when increasing the risk threshold τ. Besides, if we increase the risk threshold τ, then the risk ratio, the average time and the average number are increasing for the Green inspection channel while those three indices are decreasing for the Red inspection channel.

Nevertheless, it can be observed in Fig. 8 and Fig. 9 that the major performance measures for the whole queueing system would be neither monotonically increasing nor monotonically decreasing when varying the risk threshold. It can be seen from Fig. 8 that the safety level $SL(\tau)$ is a decreasing function of risk threshold τ. In Fig. 8, we also observe that the curves of average number $L(\tau, s_1, s_3)$ and average time $W(\tau, s_1, s_3)$ are decreasing and concave upward when the risk threshold is smaller than an inflection point, while these two curves become increasing and concave downward if the risk threshold is larger than an inflection point. In Fig. 9, it shows a closer insight into the curves of those three major performance measures when the risk threshold lies in the interval $[0\%, 25\%]$.

For more detailed discussion and application on a two-level inspection queueing model with only one risk

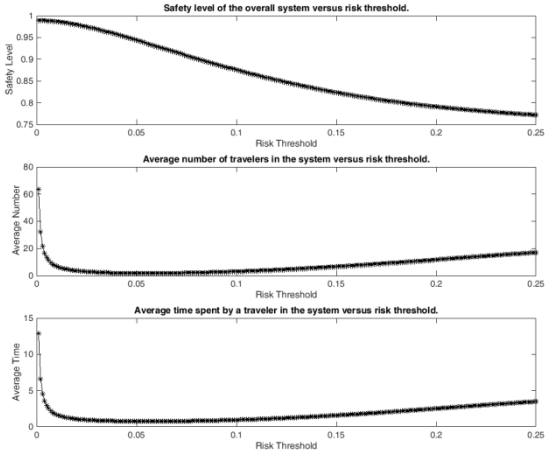

FIGURE 9. Three performance indices for a two-level inspection queueing system when varying the risk threshold between 0% and 25%.

threshold, interested readers may refer to those research works in [33]–[36] and references therein.

V. CONCLUSION

In this article, we study the queueing management on health inspection process based on a three-color risk screening mechanism at border checkpoints. We develop an analytical method for a queueing system with three levels of inspection channels to meet the need of border control during the post-COVID economic recovery. The mathematical model derived in this article is useful as a quantitative description of cross-border travelers' stochastic behaviors in order to make border control policies of government departments, and it aims to provide information about the relationships among relative factors influencing the studied queueing system.

The originality of this article lies in the formulation of a three-level inspection queueing model based on the three-color risk screening management mechanism. It is a new phenomenon and an innovative method for border control under the current prevention and control situation of the ongoing COVID-19 pandemic. The main contribution of the present work is to get a more detailed understanding of the trade-off between safety and efficiency in the epidemic prevention and control management at the border crossing checkpoints.

In the presented analysis, we formulated a three-level queueing model taking both risk and efficiency into account, and derived the equilibrium distributions of the studied queueing system under the stability conditions. Moreover, three major performance measures were derived theoretically to evaluate the proposed queueing model, including the average number of travelers to be inspected, the average time spent by each cross-border traveler, and the safety level of the overall queueing system. Furthermore, by studying a special case (when two risk thresholds were assumed to be identical), we also demonstrated that our three-level health inspection queue could be simplified to a model with two types of inspection channels and only one risk threshold, which had been widely applied in the related works on inspection process.

In the numerical results, we illustrated the monotonicity, convexity and sensitivity analysis of the studied queueing system. Through the subsequent computational experiments, it revealed some managerial insight into the three-level inspection queueing system, which could reconcile a conflict between efficiency and safety in the inspection tasks. Besides, our findings could also provide a helpful reference for implementing the prevention and control strategy more accurately classified and differentiated, especially when dredging the bottleneck points for the flow of travelers at border customs.

The application of our research work can be used in formulating feasible inspection measures for hierarchical diversion in the cross-border flow of travelers. For example, the queueing analysis conducted in this article can be applied to meet the demand of border control on improving the efficiency of inspection service while ensuring the overall safety level. Furthermore, the system performance of the border crossing points can be quantitatively evaluated and analyzed while taking into both risk and efficiency account.

In a COVID-19 world, it is necessary to scientifically carry out their border control management and accurately maintain the smooth flow of cross-border travelers. Meanwhile, it is essential to take the initiative on an orderly return to normal cross-border activities for post-COVID global economic recovery. Consequently, the mathematical analysis and performance evaluation in this article can be a scientific tool of exploring the measures for releasing cross-border travelling restriction during the current epidemic prevention and control.

REFERENCES

[1] L. Zhong, L. Mu, J. Li, J. Wang, Z. Yin, and D. Liu, "Early prediction of the 2019 novel coronavirus outbreak in the mainland China based on simple mathematical model," *IEEE Access*, vol. 8, pp. 51761–51769, 2020, doi: 10.1109/ACCESS.2020.2979599.

[2] V. Chamola, V. Hassija, V. Gupta, and M. Guizani, "A comprehensive review of the COVID-19 pandemic and the role of IoT, drones, AI, blockchain, and 5G in managing its impact," *IEEE Access*, vol. 8, pp. 90225–90265, 2020, doi: 10.1109/ACCESS.2020.2992341.

[3] Z. G. Zhang, H. P. Luh, and C.-H. Wang, "Modeling security-check queue," *Manage. Sci.*, vol. 57, no. 11, pp. 1979–1995, 2011.

[4] L. Fiondella, S. S. Gokhale, N. Lownes, and M. Accorsi, "Security and performance analysis of a passenger screening checkpoint for mass-transit systems," in *Proc. IEEE Conf. Technol. Homeland Secur. (HST)*, Nov. 2012, vol. 43, no. 4, pp. 312–318.

[5] C.-H. Wang, M.-E. Wu, and C.-M. Chen, "Inspection risk and delay for screening cargo containers at security checkpoints," in *Proc. Int. Conf. Intell. Inf. Hiding Multimedia Signal Process. (IIH-MSP)*, Adelaide, SA, Australia, Sep. 2015, pp. 211–214.

[6] V. L. Lazar Babu, R. Batta, and L. Lin, "Passenger grouping under constant threat probability in an airport security system," *Eur. J. Oper. Res.*, vol. 168, no. 2, pp. 633–644, Jan. 2006.

[7] L. A. McLay, S. H. Jacobson, and J. E. Kobza, "A multilevel passenger screening problem for aviation security," *Nav. Res. Logistics*, vol. 53, no. 3, pp. 183–197, 2006.

[8] H. Cavusoglu, B. Koh, and S. Raghunathan, "An analysis of the impact of passenger profiling for transportation security," *Oper. Res.*, vol. 58, no. 5, pp. 1287–1302, Oct. 2010.

[9] A. J. Lee and S. H. Jacobson, "Addressing passenger risk uncertainty for aviation security screening," *Transp. Sci.*, vol. 46, no. 2, pp. 189–203, May 2012.

[10] A. Parnell, K. Goniewicz, A. Khorram-Manesh, F. M. Burkle, A. Al-Wathinani, and A. J. Hertelendy, "COVID-19 a health reform catalyst?—Analyzing single-payer options in the US: Considering economic values, recent proposals, and existing models from abroad," *J. Hospital Admin.*, vol. 9, no. 4, pp. 10–19, 2020.

[11] A. L. Concho and J. E. Ramirez-Marquez, "A mathematical framework for passenger screening optimization via a multi-objective evolutionary approach," *Comput. Ind. Eng.*, vol. 62, no. 4, pp. 839–850, May 2012.
[12] A. G. Nikolaev, A. J. Lee, and S. H. Jacobson, "Optimal aviation security screening strategies with dynamic passenger risk updates," *IEEE Trans. Intell. Transp. Syst.*, vol. 13, no. 1, pp. 203–212, Mar. 2012.
[13] H. Luh, Z. G. Zhang, and C.-H. Wang, "A computing approach to two competing services with a finite buffer effect," in *Proc. 8th Int. Conf. Queueing Theory Netw. Appl. (QTNA)*, 2013, pp. 15–21.
[14] A. Bagchi and J. A. Paul, "Optimal allocation of resources in airport security: Profiling vs. Screening," *Oper. Res.*, vol. 62, no. 2, pp. 219–233, Apr. 2014.
[15] S. Wong and N. Brooks, "Evolving risk-based security: A review of current issues and emerging trends impacting security screening in the aviation industry," *J. Air Transp. Manage.*, vol. 48, pp. 60–64, Sep. 2015.
[16] A. Khorram-Manesh, E. Carlström, A. J. Hertelendy, K. Goniewicz, C. B. Casady, and F. M. Burkle, "Does the prosperity of a country play a role in COVID-19 outcomes?" *Disaster Med Public Health Preparedness*, vol. 12, pp. 1–20, Aug. 2020, doi: 10.1017/dmp.2020.304.
[17] A. Barnett, R. Shumsky, M. Hansen, A. Odoni, and G. Gosling, "Safe at home? An experiment in domestic airline security," *Oper. Res.*, vol. 49, no. 2, pp. 181–195, Apr. 2001.
[18] A. J. Lee, A. G. Nikolaev, and S. H. Jacobson, "Protecting air transportation: A survey of operations research applications to aviation security," *J. Transp. Secur.*, vol. 1, no. 3, pp. 160–184, Sep. 2008.
[19] X. Nie, G. Parab, R. Batta, and L. Lin, "Simulation-based selectee lane queueing design for passenger checkpoint screening," *Eur. J. Oper. Res.*, vol. 219, no. 1, pp. 146–155, May 2012.
[20] C.-H. Wang and J. Lan, "Performance evaluation of a risk-based three-tier inspection system," *DEStech Trans. Comput. Sci. Eng.*, pp. 464–468, Dec. 2017. [Online]. Available: http://dpi-proceedings.com/index.php/dtcse/article/view/16417, doi: 10.12783/dtcse/cmsam2017/16417.
[21] G. J. Hanumantha, B. T. Arici, J. A. Sefair, and R. Askin, "Demand prediction and dynamic workforce allocation to improve airport screening operations," *IISE Trans.*, vol. 52, no. 12, pp. 1324–1342, 2020, doi: 10.1080/24725854.2020.1749765.
[22] J. E. Kobza and S. H. Jacobson, "Probability models for access security system architectures," *J. Oper. Res. Soc.*, vol. 48, no. 3, pp. 255–263, Dec. 1997.
[23] E. H. Kaplan, "Terror queues," *Oper. Res.*, vol. 58, no. 4, pp. 773–784, 2010.
[24] R. de Lange, I. Samoilovich, and B. van der Rhee, "Virtual queuing at airport security lanes," *Eur. J. Oper. Res.*, vol. 225, no. 1, pp. 153–165, Feb. 2013.
[25] L. Lin, Q. Wang, and A. W. Sadek, "Border crossing delay prediction using transient multi-server queueing models," *Transp. Res. Part A, Policy Pract.*, vol. 64, pp. 65–91, Jun. 2014.
[26] C.-H. Wang and X. Wu, "Performance analysis of a security-check system with four types of inspection channels for high-speed rail stations in China," in *Smart Service Systems, Operations Management, and Analytics*, H. Yang, R. Qiu, and W. Chen, Eds. Nanjing, China: Springer, 2019, pp. 7–16.
[27] C.-H. Wang and H. P. Luh, "Estimating the loss probability under heavy traffic conditions," *Comput. Math. Appl.*, vol. 64, no. 5, pp. 1352–1363, Sep. 2012.
[28] A. Seidl, E. H. Kaplan, J. P. Caulkins, S. Wrzaczek, and G. Feichtinger, "Optimal control of a terror queue," *Eur. J. Oper. Res.*, vol. 248, no. 1, pp. 246–256, Jan. 2016.
[29] A. J. Lee and S. H. Jacobson, "The impact of aviation checkpoint queues on optimizing security screening effectiveness," *Rel. Eng. Syst. Saf.*, vol. 96, no. 8, pp. 900–911, Aug. 2011.
[30] K. D. Majeske and T. W. Lauer, "Optimizing airline passenger prescreening systems with Bayesian decision models," *Comput. Oper. Res.*, vol. 39, no. 8, pp. 1827–1836, Aug. 2012.
[31] The State Council of the People's Republic of China, "The epidemic prevention health information code," Nat. Government Service Platform, Beijing, China, Tech. Rep., 2020. [Online]. Available: http://gjzwfw.www.gov.cn/col/col641/index.html
[32] L. A. McLay, A. J. Lee, and S. H. Jacobson, "Risk-based policies for airport security checkpoint screening," *Transp. Sci.*, vol. 44, no. 3, pp. 333–349, Aug. 2010.
[33] C.-H. Wang, "A modelling framework for managing risk-based checkpoint screening systems with two-type inspection queues," in *Proc. 3rd Int. Conf. Robot, Vis. Signal Process. (RVSP)*, Kaohsiung, Taiwan, Nov. 2015, pp. 220–223.
[34] C.-H. Wang, "Arena simulation for aviation passenger security-check systems," in *Genetic and Evolutionary Computing* (Advances in Intelligent Systems and Computing), vol. 536. Cham, Switzerland: Springer, 2016, pp. 95–102.
[35] C.-H. Wang, "A queueing analysis of a security-check system with two types of inspection channels," in *Proc. Int. Conf. Math., Modelling, Simulation Algorithms (MMSA)*, in Advances in Intelligent Systems Research, vol. 159. Amsterdam, The Netherlands: Atlantis Press, 2018, pp. 102–106.
[36] C.-H. Wang, "A matrix-analytic method for evaluating performance of security-check system with two-type inspection queues," in *Proc. Int. Conf. Ind. Eng. Syst. Manage. (IESM)*, Shanghai, China, Sep. 2019.

CHIA-HUNG WANG (Member, IEEE) received the B.S. degree in mathematics from National Tsing Hua University, Hsinchu, Taiwan, in 2002, the M.S. degree in mathematical sciences from National Chengchi University, Taipei, Taiwan, in 2004, and the Ph.D. degree in operations research from the Department of Mathematical Sciences, National Chengchi University, in 2011.

He visited the University of Illinois at Chicago, USA, as a Visiting Scholar, from August 2007 to August 2008. From 2011 to 2015, he was a Postdoctoral Fellow with National Chiao Tung University and National Cheng Kung University, Taiwan. Since 2015, he has been with the College of Information Science and Engineering, Fujian University of Technology, China, where he currently holds an Associate Professor position. Meanwhile, he also serves as a Research Fellow with the Fujian Provincial Key Laboratory of Big Data Mining and Applications, China. He is also an Expert in operations research, applied mathematics, information systems, and data science. He has been involved in several collaborative projects with international professionals, including the modeling and analysis of security-check queues, the management mechanisms for service systems, and the design of management schemes on communication networks. These research works have already been published in over 60 refereed journals and conference proceedings, including *Management Science*, *Soft Computing*, *Computers and Operations Research*, IEEE Access, *Computers and Mathematics with Applications*, *International Journal of Information and Management Sciences*, and so on.